The Melting Effect as a Factor in Precipitation-Type Forecasting

JOHN S. KAIN

Cooperative Institute for Mesoscale Meteorological Studies, and NOAA/OAR/National Severe Storms Laboratory, Norman, Oklahoma

STEPHEN M. GOSS

NOAA/NWS/Storm Prediction Center, Norman, Oklahoma

MICHAEL E. BALDWIN

Cooperative Institute for Mesoscale Meteorological Studies, NOAA/OAR/National Severe Storms Laboratory, and NOAA/NWS/Storm Prediction Center, Norman, Oklahoma

(Manuscript received 11 January 2000, in final form 20 June 2000)

ABSTRACT

The process of atmospheric cooling due to melting precipitation is examined to evaluate its contribution to determining precipitation type. The ''melting effect'' is typically of second-order importance compared to other processes that influence the lower-tropospheric air temperature and hence the type of precipitation that reaches the ground. In some cases, however, cooling due to melting snowflakes can emerge as the dominant agent of temperature change, occasionally surprising forecasters (and the public) by inducing an unexpected changeover from rain to heavy snow. One such case occurred on 3–4 February 1998 in east-central Tennessee and surrounding areas.

Commonly applied considerations for predicting precipitation type had convinced forecasters that significant snowfall was not likely with this event. However, real-time observations and a postevent analysis by forecasters at the Storm Prediction Center led to the hypothesis that the melting effect must have provided the cooling necessary to allow widespread heavy snowfall. To test this hypothesis, the Pennsylvania State University–NCAR Mesoscale Model was used to generate a mesoscale-resolution, four-dimensional dataset for this event. Diagnostic analysis of the model output confirmed that cooling due to melting snowflakes was of a sufficient magnitude to account for the disparity between observed and forecasted lower-tropospheric temperatures in this case.

A simple formula is derived to provide a ''rule of thumb'' for anticipating the potential impact of the melting effect. In addition, guidelines are provided for identifying meteorological patterns that favor a predominance of the melting effect.

1. Introduction

Frozen precipitation begins to melt if it passes through above-freezing air on its trajectory to the surface. Since the melting process extracts heat from the surrounding environment, this process introduces a cooling tendency throughout the layer where melting occurs, a layer that is typically several hundred meters deep (e.g., Braun and Houze 1995). A persistent melting process can cool the temperature of the ambient air to 0°C (at which point melting stops), allowing subsequent hydrometeors to fall farther before melting completely. This effect promotes a gradual downward propagation of melting-induced cooling and, *when temperature tendencies associated with other processes are relatively small*, it can create an isothermal layer with a temperature of 0°C (e.g., Findeisen 1940).

This characteristic isothermal layer does not always form when hydrometeors melt because in most precipitating atmospheres other processes mask the effect of melting. For example, cooling associated with melting precipitation is typically smaller in magnitude than other latent heating effects (i.e., condensation and evaporation) because the latent heat of vaporization (L_v) is nearly an order of magnitude larger than the latent heat of fusion (L_f). This disparity is mitigated somewhat by the fact that the melting process tends to be concentrated in a relatively shallow layer and it typically involves *all* of the precipitation, while evaporation is spread over a deeper layer and ends up being an incomplete process when precipitation reaches the surface. Nonetheless, a dominance of melting effects over evaporative cooling

Corresponding author address: Dr. John S. Kain, National Severe Storms Laboratory, 1313 Halley Circle, Norman, OK 73069.
E-mail: kain@nssl.noaa.gov

would probably be limited to those environments where precipitation was falling through a nearly saturated environment (little or no potential for evaporation) where vertical motions are weak (no support for active condensation or subsidence-induced drying). Moreover, even if melting becomes the dominant *latent heating* effect in a layer, its impact can be overshadowed by temperature advections (both vertical[1] and horizontal). Thus, the melting effect and its impact are often difficult to discern.

With careful examination of data, however, the dynamical consequences of melting can be detected in some environments. The cooling tendency due to melting is directly proportional to the precipitation rate, so that melting effects are felt most strongly where precipitation rates are high. A natural consequence of temperature anomalies generated by melting of locally heavy precipitation is the induction of mesoscale dynamical perturbations. Hydrostatic mesoscale pressure perturbations associated with melting effects can induce perturbations in the wind field along the path of precipitation-rate maxima (Atlas et al. 1969). Pressure perturbations caused by melting effects can also have a significant impact on flow patterns and precipitation rates in orographic precipitation events (Marwitz 1983; Marwitz and Toth 1993). Cooling due to melting can also modify significantly frontal circulations and enhance frontogenesis, especially when the melting layer is near the ground (Carbone 1982; Marwitz and Toth 1993; Szeto and Stewart 1997).

Of course, when the melting layer is close to the ground, a significant concern for forecasters becomes whether or not frozen precipitation can reach the surface (Lumb 1961). In some cases, the melting effect can become an important consideration in the accurate prediction of precipitation type. In particular, when condensation, evaporation, and advective effects are weak in the lower troposphere, but precipitation rates are at least moderately high, a 0°C isothermal layer can form, as described above. The formation of this feature effectively moves the melting layer closer to the surface and increases the likelihood that snow will reach the ground. In extreme cases, such isothermal layers can extend down as much as 3 km underneath the original melting level (Stewart 1992), although more typically, they are observed to be on the order of 1 km deep (Stewart 1984). In some situations, the depth of the isothermal layer varies horizontally as a function of precipitation rate, so that snow is observed at the surface where precipitation rates are high (because the isothermal layer grows deeper), but rain falls in surrounding areas where the intensity is lower (Wexler et al. 1954; Gedzelman and Lewis 1990; Ferber et al. 1993). Likewise, in regions of steep terrain, snow levels can descend where precipitation rates are high (e.g., Steenburgh et al. 1997).

A particularly challenging task for forecasters is to anticipate when melting effects might influence the type of precipitation observed at the surface. At any given location, cooling due to melting appears to make the difference between rain and snow quite rarely, so the potential significance of melting is often neglected in the forecast preparation process—typically without egregious error. During those infrequent events when melting *does* become a pivotal factor, however, forecasters and the public can be caught by surprise. Furthermore, since a melting-induced changeover to snow is promoted by high precipitation rates, resulting snowfalls can be heavy and the consequences of a poor forecast can be exceptionally serious.

One such event took place on 3–4 February 1998 over the midsouth region of the United States (east-central Tennessee and surrounding areas). With this storm, locally heavy rainfall was followed by an unexpected changeover to snow and accumulations of over 30 cm (1 ft) of snow in some locations. An examination of this event is used for a fourfold purpose. First, the evolution of this weather system is presented from a forecaster's perspective in order to show how difficult it was to anticipate the changeover to snow that occurred, while also showing that evidence for the possible role of the melting effect mounted during the forecast shift and a postevent analysis. Second, it is shown how a numerical forecast model can be used as a diagnostic tool to confirm and quantify the impact of melting precipitation on lower-tropospheric thermodynamic structure. Third, quantitative guidance is offered to assist forecasters in predicting when cooling due to melting might become a significant factor in forecasting precipitation type. Fourth, it is argued that this study was greatly facilitated by the convenience afforded by the collocation of the National Severe Storms Laboratory (NSSL) and the Storm Prediction Center (SPC) and daily interactions between forecasters and research scientists that occur at this facility.

In the next section, an observational summary of the 3–4 February 1998 event is presented. This is followed by a diagnostic analysis of the evolution of thermodynamic structures and the physical processes responsible for this evolution using a numerical weather prediction model. Next, a simple formula for estimating the potential impact of melting is derived and guidelines for its operational implementation are proposed, followed by concluding remarks.

2. Observations

During the early afternoon of 3 February 1998, a 992-mb surface low was moving northeastward across the

[1] In this study, ''vertical advection'' of temperature denotes the adiabatic temperature change associated with vertical motions, which can be expressed as $\partial T/\partial t = -w(\Gamma_d - \gamma)$, where T is temperature (K), t is time (s), w is vertical velocity (m s^{-1}), Γ_d is the dry-adiabatic lapse rate (K s^{-1}), and γ is the actual lapse rate (K s^{-1}).

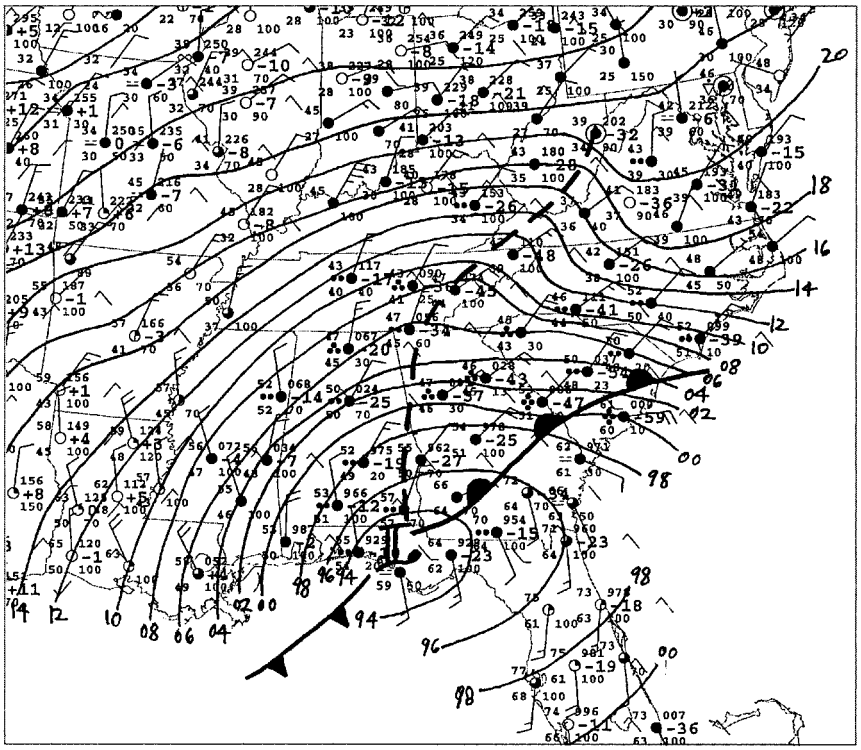

FIG. 1. Surface observational analysis valid 1800 UTC 3 Feb 1998. Sea level pressure is contoured in 2-mb increments. Station model and frontal analyses are standard.

Florida panhandle toward southern Georgia (Fig. 1). This low was the surface reflection of a well-developed cyclone, with closed height contours extending from the surface through the middle troposphere in a nearly vertical configuration. At 850 mb, 1200 UTC data indicated a large cyclonic circulation over the southeastern United States with generally mild temperatures (Fig. 2a). Over the Tennessee Valley region, where a broad shield of rain had moved in during the morning hours, 850-mb temperatures (and wet-bulb temperatures as will be shown later in Fig. 7b) were well above freezing and cold air advection appeared to be weak at 1200 UTC. At 500 mb the disturbance was manifested as a negatively tilted trough over the southeastern United States (Fig. 2b). The circulation patterns through this trough contributed to a broad swath of warm advection extending from the Florida panhandle north-northwestward to the Midsouth region. The precipitation observed on the eastern and northern sides of the surface low was associated with this ''conveyor belt'' airflow (Carlson 1991).

The 1200 UTC sounding from Nashville, Tennessee (BNA), showed northeasterly flow extending from the surface to near 600 mb, with winds veering to southerly and southwesterly above this level (Fig. 3). The atmosphere was apparently saturated (with respect to ice) above about 600 mb, while it was quite moist, but generally subsaturated below this level. The 0°C wet-bulb temperature was about 200 mb above the surface.

During the afternoon, National Weather Service forecasts for the Tennessee Valley region called for a continuation of the rainfall with temperatures in the upper 30s and lower 40s (°F).[2] Surface data valid 2100 UTC (Fig. 4a) showed that temperatures were generally in the mid 40s over the region, although London, Kentucky (LOZ), and Jackson, Kentucky (JKL), which are located in higher elevation areas of the Cumberland Plateau, were in the upper 30s.

In contrast to the forecasts, however, rapid changes in the surface weather occurred between 2200 and 0200 UTC (Figs. 4b–f). During this time across middle and eastern Tennessee and eastern Kentucky, temperatures fell into the low 30s and observed weather changed from rain to snow in many locations, with moderately heavy snowfall rates common. For example, BNA, the changeover to snow was accompanied by a surface temperature drop from 44°F at 2200 UTC to 34°F at 0200 UTC. By the end of the event, after midnight on 4 February, as much as 1 ft of unexpected snowfall blanketed parts of middle and eastern Tennessee, with lesser amounts in surrounding areas. Numerous trees were brought down by the heavy, wet snow, and thousands of power outages were reported across the region.

[2] In this section surface temperatures are expressed in units of degrees Fahrenheit since these are the standard units used by National Weather Service forecasters.

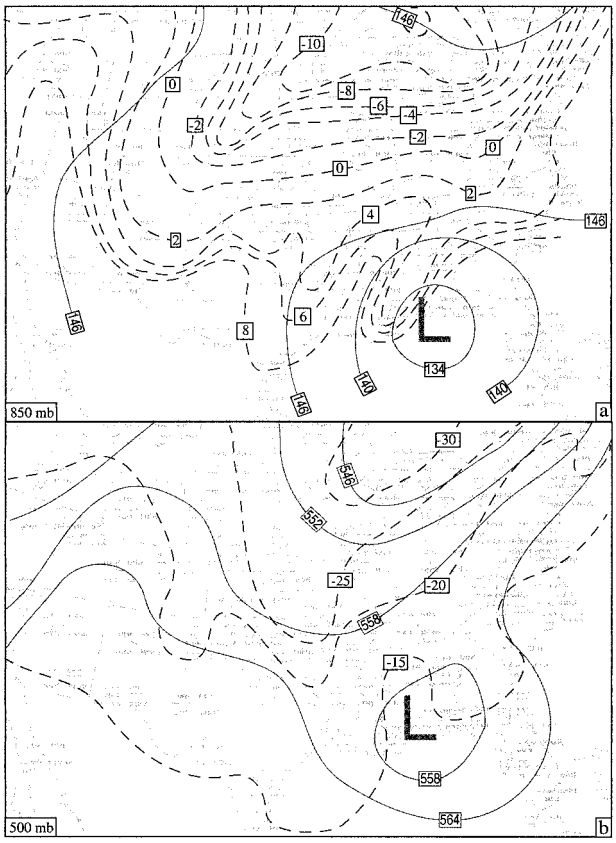

FIG. 2. Upper-air observational analyses valid 1200 UTC 3 Feb 1998: (a) 850 and (b) 500 mb. Solid lines are contours of geopotential height (every 6 dam) and dashed lines are contours of temperature (every 2°C).

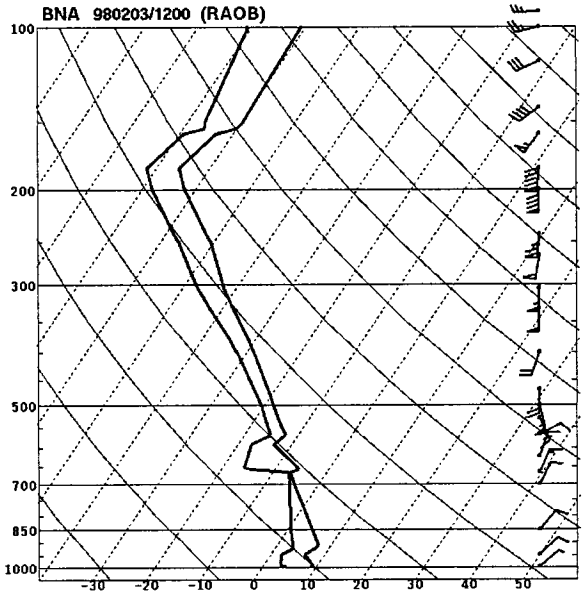

FIG. 3. Observed sounding from BNA plotted on a standard skew *T*–log*p* diagram, valid 1200 UTC 3 Feb 1998.

At the SPC, forecasters working the Mesoscale Forecast desk also did not anticipate the rapidly changing weather conditions. However, over the course of the forecaster shift, SPC forecasters compiled evidence that helped them form a hypothesis regarding the physical processes that led to the unexpected snowstorm. After a thorough postevent analysis of the case, several additional details were revealed. In particular, the following observations were considered to be relevant to developing an understanding of this event.

1) The closest below-freezing air in the lower troposphere (i.e., at the 850- and 925-mb levels) was several hundred kilometers away from eastern and central Tennessee at 1200 UTC. Although weak cold advection was occurring across the region at this time, winds were expected to veer during the day, suggesting that cold advection would probably be insufficient to lower temperatures to freezing.
2) The observed surface temperature falls occurred *only* in areas where persistent precipitation was occurring, with a sharp temperature gradient noted along the edge of the precipitation shield. This would imply that the precipitation was somehow involved in the observed cooling, but since observed soundings were nearly saturated (e.g., Fig. 5), appreciable evaporative cooling seemed unlikely.
3) The observed 0000 UTC 4 February sounding from BNA showed a near-freezing isothermal layer between approximately 850 and 925 mb (Fig. 5). This feature was not present in the 1200 UTC 3 February sounding. In fact, the lowest 250 mb of the sounding was above freezing at the earlier time (Fig. 3). As suggested in the introduction, snow melting through a warmer layer of the atmosphere would introduce a cooling tendency that could draw ambient temperatures toward the freezing point. Upper portions of the melting layer would probably reach 0°C first, creating an environment that would allow snowflakes to fall farther before melting completely and allowing melting-induced cooling to descend to lower elevations. If sufficient precipitation were to fall, an entire warm layer could eventually be eroded in this way, resulting in a near-freezing isothermal layer where a melting layer once existed.
4) A radar bright band was observed (higher reflectivity resulting from frozen precipitation beginning to melt, presumably near the top of the melting layer). This bright band was observed to shrink toward the KBNA radar with time (Fig. 6), implying that the top of the melting layer was progressively moving to lower elevations with time. This observation was consistent with a process involving cooling of the lower layers of the atmosphere from above, as suggested by the 0000 UTC sounding (Fig. 5).
5) Surface observations showed temperatures falling as low as 32°F (0°C) but *no lower*. This would be expected in a situation where cooling was occurring as

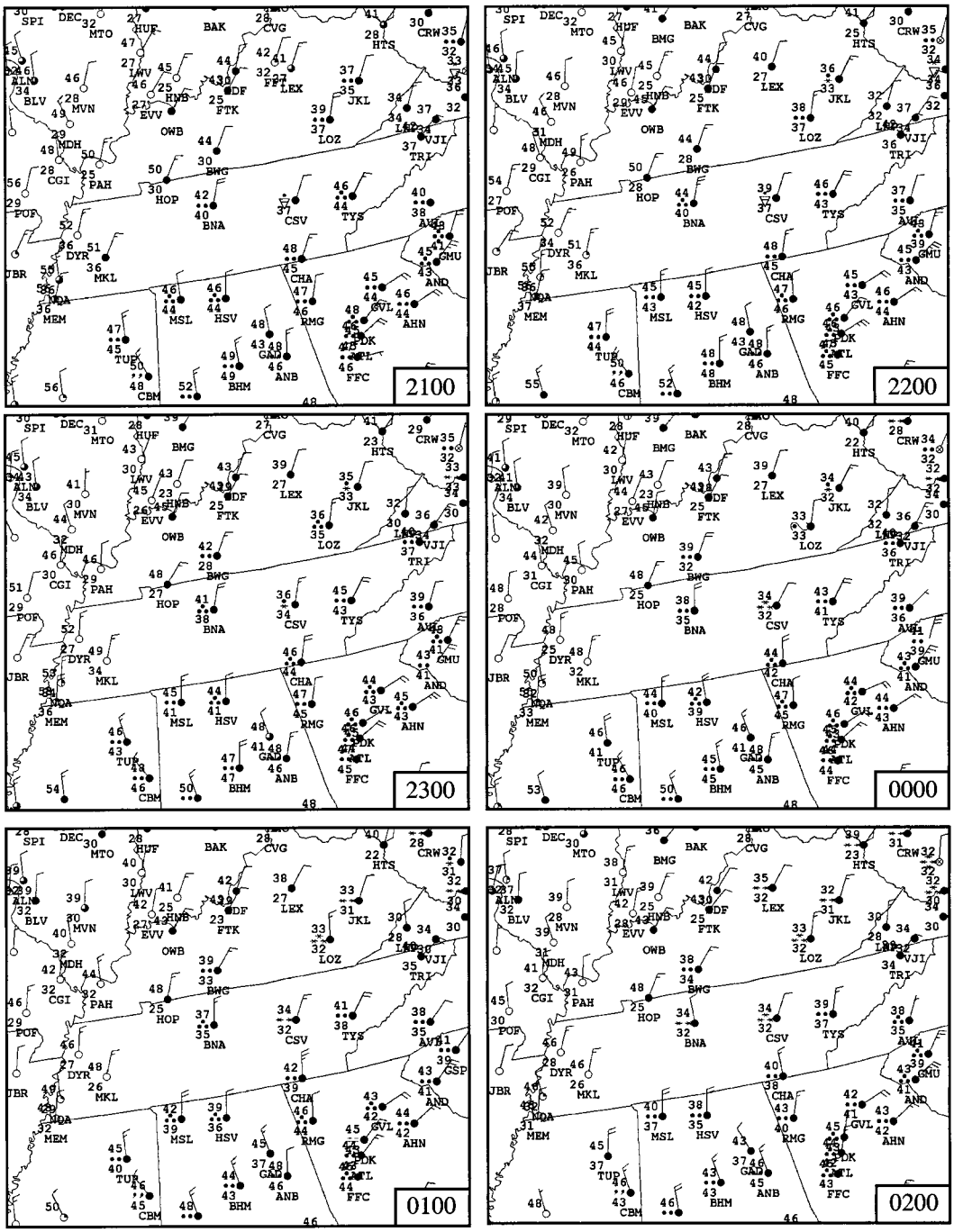

FIG. 4. Hourly surface observations valid (a) 2100, (b) 2200, and (c) 2300 UTC 3 Feb and (d) 0000 (e) 0100, and (f) 0200 UTC 4 Feb 1998. Station model is standard.

a result of melting. Removal of heat from the atmosphere to allow melting to occur could cool the atmosphere to the freezing point. Once the atmosphere cooled to this point, melting would obviously cease, along with the associated cooling.

6) As mentioned, the precipitation was significant in both intensity and duration. Moderate to heavy, persistent precipitation would be required to erode a deep warm layer. A break in the precipitation would cause cooling to cease.

Collectively, these observations led to the following hypothesis: *latent heat absorption aloft during the endothermic phase change that occurred as snowflakes*

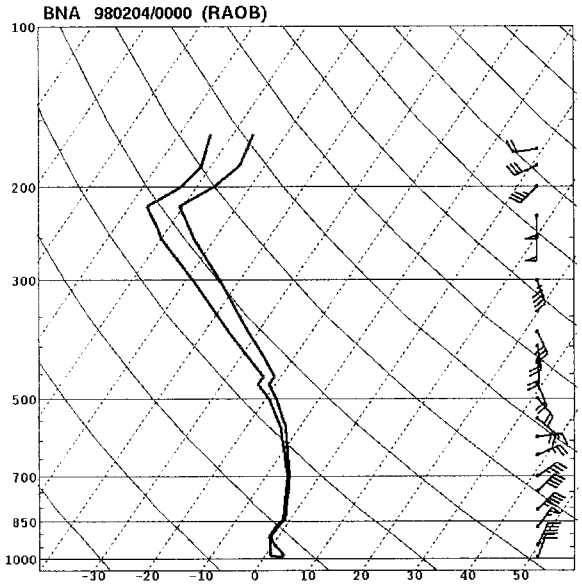

FIG. 5. Observed sounding from BNA plotted on a standard skew *T*–log*p* diagram, valid 0000 UTC 4 Feb 1998.

fell into a layer of above-freezing air and melted into raindrops was likely a primary contributor to atmospheric cooling. This process eventually led to the observed rapid surface temperature falls and a subsequent changeover from rain to snow at the ground. In order to substantiate this hypothesis, the Pennsylvania State University–National Center for Atmospheric Research fifth-generation Mesoscale Model (MM5; Grell et al. 1994; Dudhia 1993) was utilized as a diagnostic tool for this case. Results from the model diagnostics will be discussed in the next section.

3. Diagnostic analysis using a numerical model

At the NSSL, MM5 is run on a daily basis on a 10-processor SGI Power Challenge workstation. Output from the higher-resolution domain, which covers the eastern two-thirds of the United States, is posted on the World Wide Web. These daily runs derive initial conditions from the 0000 UTC Eta Model (Black 1994) analysis, simply interpolating the Eta Model fields to the MM5 grid points. Consequently, data acquisition procedures are dependable and efficient and output for a 48-h integration is typically posted by 0700 UTC, in plenty of time to make it useful for the forecast process.

In addition to its utility as a forecasting tool, the ready availability of this dataset and the ease with which this modeling system can be rerun also make it very attractive for research purposes. Detailed diagnostic calculation of model output fields can easily be performed and additional diagnostics can readily be inserted for reruns of the model, facilitating the use of this modeling system as a timely diagnostic tool for use by research scientists and forecasters at NSSL and the SPC.

For this study, this ''real time'' configuration and initialization procedure was used in order to demonstrate the utility of this prediction model as a diagnostic tool in an operational setting. A cursory comparison of the model simulation and observations are provided below to establish the validity of the model output as a diagnostic dataset.

a. Model description

The model configuration includes the following:

- a 90-km grid length on the large domain (not shown here) and a 30-km grid length on the inner domain, with 23 vertical levels (~30 mb grid interval in the melting layer);
- a high-resolution planetary boundary layer parameterization (Zhang and Anthes 1982);
- the Kain–Fritsch convective parameterization (Kain and Fritsch 1993);
- parameterized surface and atmospheric radiation processes (Dudhia 1989); and
- an explicit, bulk parameterization of microphysical processes, including the ice phase and prognostic equations for cloud water/ice as well as rain/snow (Dudhia 1989).

The microphysical parameterization includes the ice phase, but does not allow mixed-phase hydrometeors. In particular, hydrometeors are assumed to be frozen at temperatures below 0°C and to be liquid above the freezing point. As will be shown below, this model configuration and its initial condition fields are adequate for the diagnostic applications of this study.

b. Model validation

Numerical simulations are initialized at 1200 UTC 3 February 1998. The initial surface pressure field shows a deep low pressure center over the Gulf of Mexico, just south of the western Florida panhandle (Fig. 7a). North of this system, a moderately strong pressure gradient exists over the southeastern states and extends up into the Ohio Valley, with northeast winds at low levels over most of this region. Temperatures are above freezing over the Southeast and range from about 4° to 8°C over Tennessee. At the 850-mb level, the freezing line is well north of Tennessee and winds are blowing nearly parallel to the gradient of *wet-bulb* temperature (Fig. 7b). These initial conditions are in reasonably good agreement with observations (Figs. 1 and 2a).

Our validation of the model simulation begins with the precipitation field. Broad-scale precipitation patterns for a 24-h simulation, ending 1200 UTC 4 February, agree quite well with observations (cf. Figs. 8a and 8b). Over Tennessee, a band of heavy precipitation (greater than 25 mm, or 1 in.) covers much of the middle and eastern parts of the state, with a sharp northwest edge close to BNA in both the forecast and observations. The

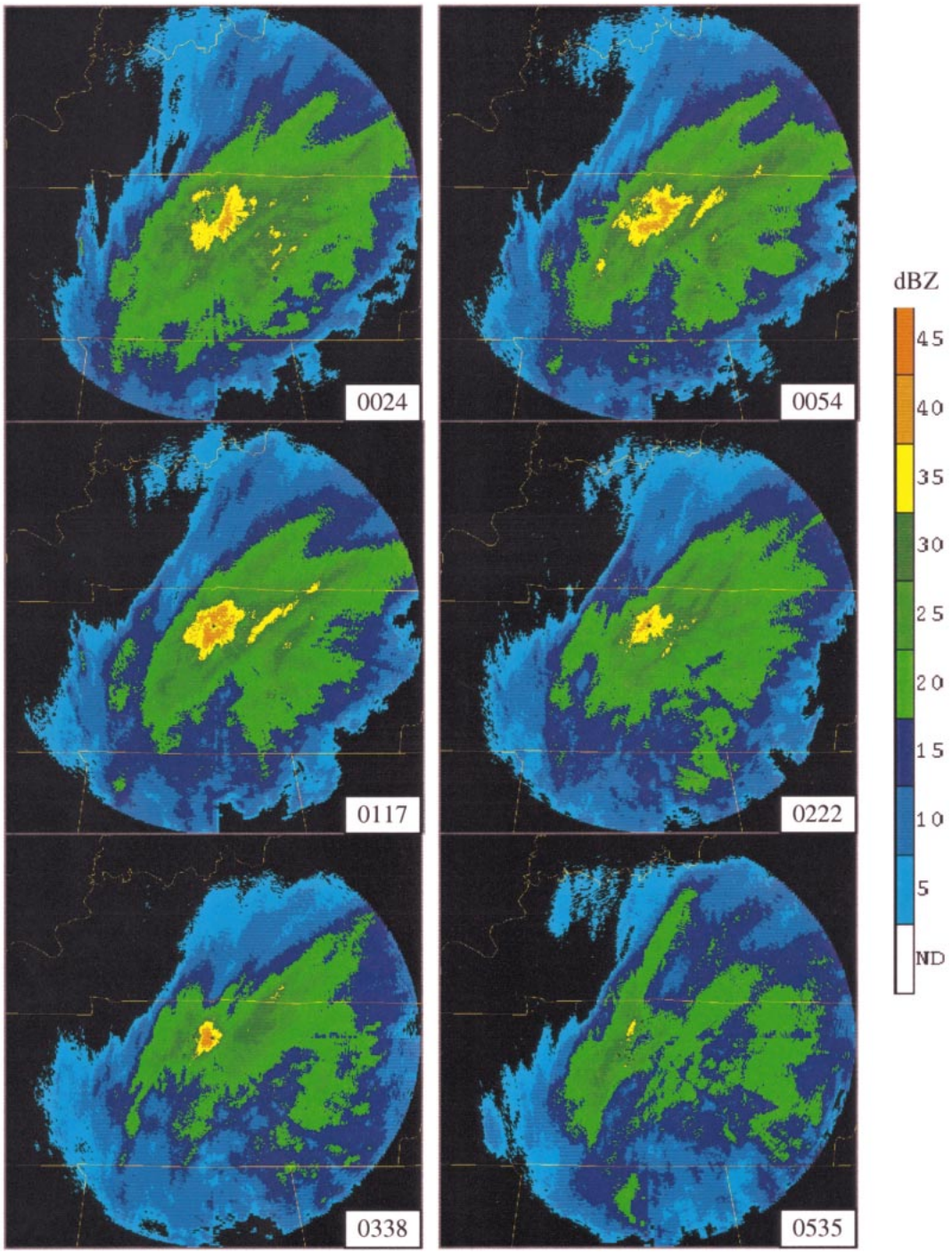

FIG. 6. Time series of base reflectivity images from KOHX (Nashville, TN) WSR-88D radar at 0.5° elevation angle. Note the shrinking with time of the ''bright band,'' or higher reflectivity region roughly surrounding the radar site.

model tends to underestimate precipitation totals over the east-central and south-central parts of the state, perhaps by as much as a factor of 2, but the good agreement in the general patterns suggests that the model has reproduced well the large-scale processes that were responsible for heavy precipitation in the region.

Further validation of the model is provided by plots of simulated surface and 850-mb patterns, valid 0000 UTC 4 February (Figs. 9a,b). The surface low pressure center and the character of the broader-scale sea level pressure field compare well with observational analyses (broader-scale observations not shown at this time, but

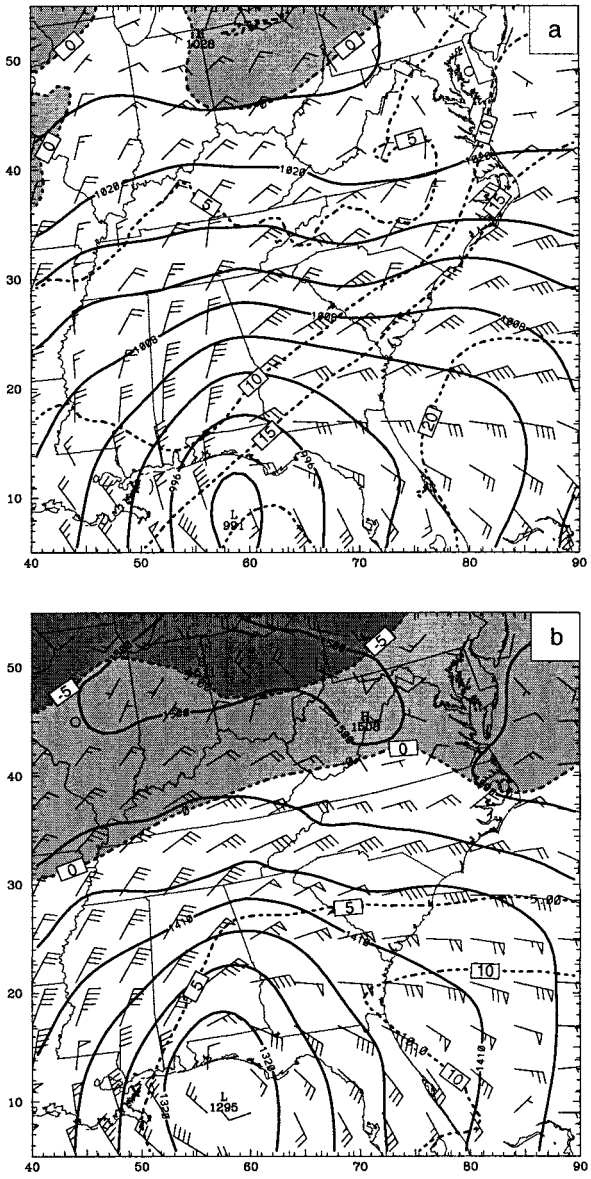

FIG. 7. Initial conditions for the MM5 simulation, valid 1200 UTC 3 Feb 1998: (a) sea level pressure (thick solid lines, contour interval = 4 mb), lowest model level wind barbs (full barb = 5 m s^{-1}), and temperature (dashed lines, contour interval = 5°C), and (b) 850-mb geopotential height (thick solid lines, contour interval = 30 m), wind barbs, and *wet-bulb* temperature (dashed lines, contour interval = 5°C). Light shading indicates temperatures between 0° and −5°C, darker shading less than −5°C.

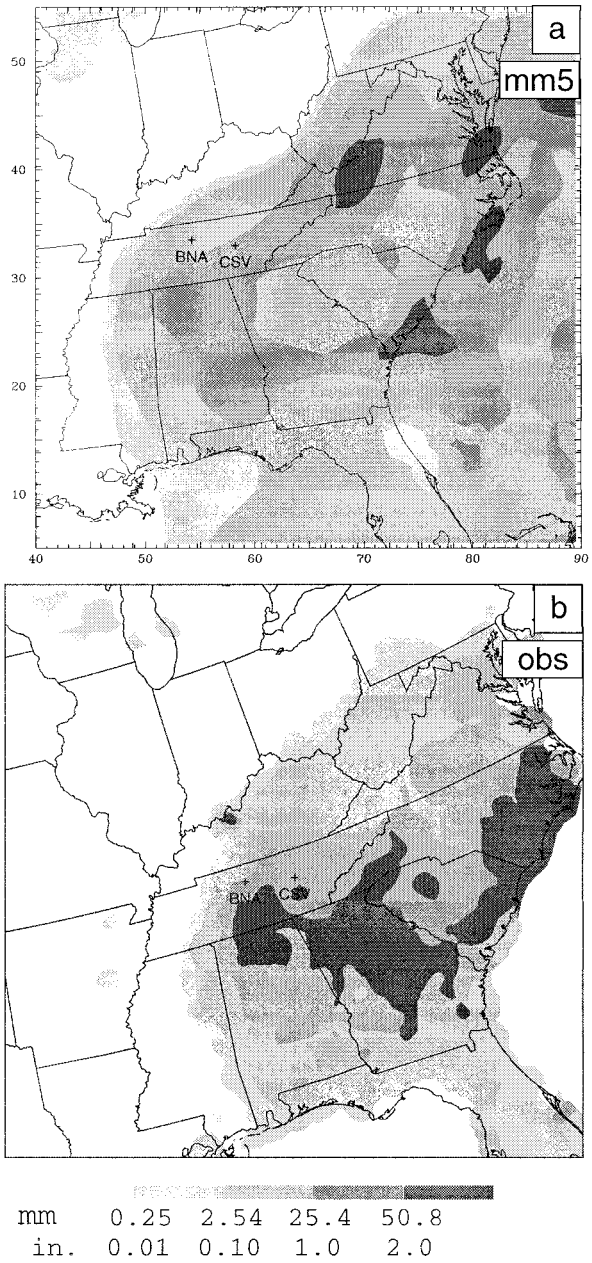

FIG. 8. The 24-h precipitation totals (mm) for the period ending 1200 UTC 4 Feb 1998 from (a) the MM5 simulation and (b) analysis of observations from the National Weather Service's River Forecast Centers.

see Fig. 1 for 1800 UTC observations). In particular, the low pressure center is positioned near Tallahassee, Florida, and a moderately strong pressure gradient covers much of the southeastern United States, including the Tennessee Valley. At 850 mb (Fig. 9b), a narrow tongue of below-freezing air extends down the backbone of the Appalachians southward into northeastern Alabama. Over Tennessee, both BNA, in the north-central part of the state, and Crossville (CSV) in the east-central region, are close to the freezing line. Although the smaller-scale features in this temperature field predicted by the model cannot be resolved by the observational network, the general agreement between observations (Fig. 10) and model predictions (Fig. 9b) appears to be quite good.

A more substantial validation of the model over the Tennessee region is given by a comparison of observed and predicted 0000 UTC soundings at BNA. The ther-

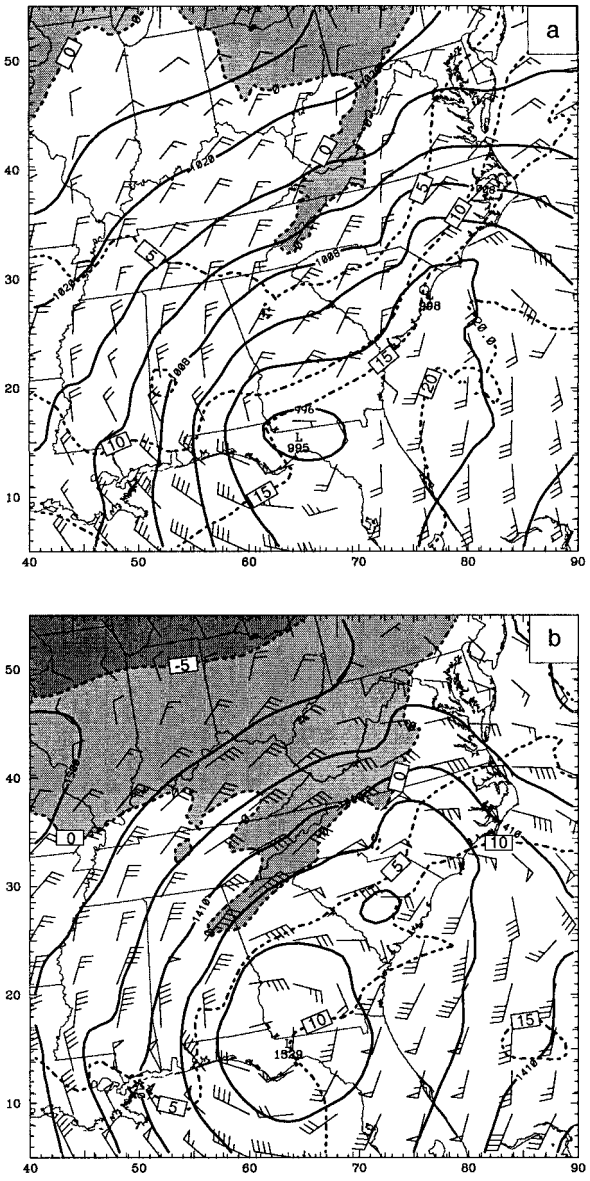

FIG. 9. Results from the 12-h time of the MM5 simulation, valid 0000 UTC 4 Feb 1998: (a) sea level pressure (thick solid lines, contour interval = 4 mb), lowest model level wind barbs (full barb = 5 ms^{-1}), and temperature (dashed lines, contour interval = 5°C), and (b) 850-mb geopotential height (thick solid lines, contour interval = 30 m), wind barbs, and temperatures as in (a). Shading as in Fig. 7.

mal structure in the model-predicted sounding (Fig. 11) contains several prominent features that are consistent with both the observed sounding (Fig. 5) and an active melting process. Most significantly, both soundings 1) are saturated over nearly the entire troposphere, consistent with appreciable precipitation rates at the surface; 2) contain a 0°C isothermal layer, roughly between 850 and 900 mb; and 3) have a relatively warm, nearly dry-adiabatic layer between the base of the isothermal layer and the ground. These comparisons suggest that the

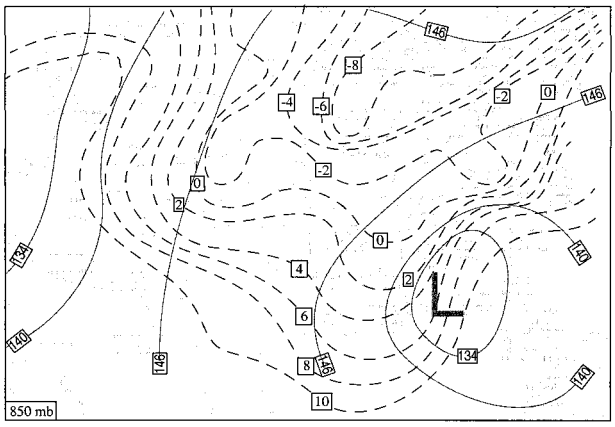

FIG. 10. Observational analysis at 850 mb, valid 0000 UTC 4 Feb 1998. Solid lines are contours of geopotential height (every 6 dam) and dashed lines are contours of temperature (every 2°C).

model simulates the dynamical and physical processes associated with this event with sufficient accuracy that we are justified in using the model as a diagnostic tool. In the following subsection, the impact of the melting effect is diagnosed using model output.

c. Model interrogation

For a closer examination of the model output, we focus attention away from BNA and eastward to CSV. The reason for this is that BNA is on the back edge of the precipitation shield and rainfall rate decreases sharply and prematurely at around 0000 UTC in the model simulation. In contrast, CSV is located within the band of heavier and more persistent rainfall. Observations

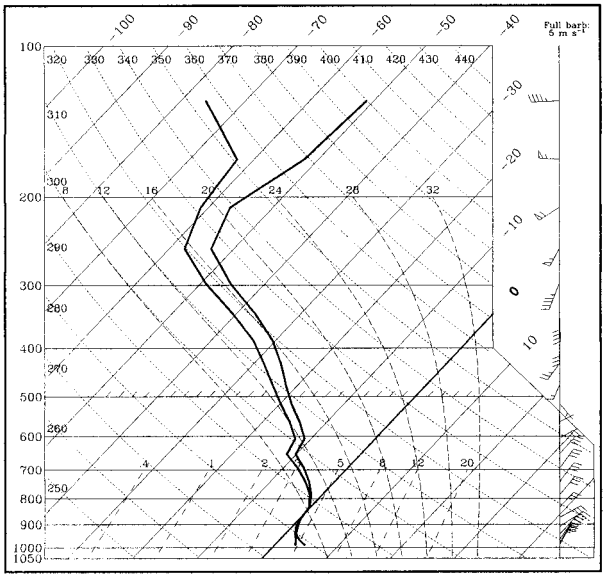

FIG. 11. Model-simulated sounding from BNA at the 12-h time, valid 0000 UTC 4 Feb 1998.

indicated that rain at CSV had changed to moderate snow by 0000 UTC (note that the elevation at CSV is about 1300 ft, or ~400 m, higher than at BNA), so we are particularly interested in interrogating the model fields near CSV during the first 12 h of the simulation.

At grid points near CSV, steady precipitation began in the model at about 1600 UTC 3 February (4 h into the simulation). Precipitation rates climbed to about 5 mm h^{-1} (0.2 in. h^{-1}) by 2000 UTC, then dropped off to about 2 mm h^{-1} (0.08 in. h^{-1}) by 0000 UTC 4 February.

1) SENSITIVITY TESTS

By the time the simulated precipitation reached its peak intensity, around 2000 UTC, a prominent isothermal 0°C layer had developed between 750 and 850 mb (Fig. 12a). A simple way to assess the impact of melting snow in generating this layer is to change the value of the latent heat of fusion, L_f, when it is used to compute the temperature change due to melting. When L_f is set to zero and the simulation is repeated with an otherwise identical model configuration, the isothermal layer does not develop (Fig. 12b). In contrast, when L_f is doubled, the isothermal layer grows deeper, extending down to about 880 mb (Fig. 12c). By 0000 UTC, the melting level had penetrated to within about 30 mb of the surface in the control simulation (Fig. 13a) and all the way to the surface layer when L_f was doubled (Fig. 13b). These experiments provide compelling evidence that the melting effect is playing a dominant role in the development and depth of this feature.

For this event, doubling the value for L_f is a particularly interesting test because it allows us to speculate how strong the melting effect would have been *if* twice as much precipitation had fallen near CSV (recall that the model actually underpredicted the total precipitation by about a factor of 2). There is some quantitative value to this estimate because, as will be shown below, almost all of the precipitation was generated well above the 0°C level over the region in question. Thus, the dynamic processes that led to the production of precipitation aloft appear to have been decoupled from the air mass in the lower troposphere (i.e., the lowest ~300 mb). It is this lower tropospheric air mass, and the degree to which it is modified by precipitation falling from overhead, that determine whether or not frozen precipitation can reach the ground. This sensitivity test allows us to speculate that, if mid- to upper-tropospheric circulations in the model had produced as much precipitation as was observed, the freezing level could have descended to the surface as was observed at CSV.

2) DIAGNOSTIC ANALYSIS OF THE CONTROL RUN

Sensitivity tests in a model (i.e., artificially manipulating physical processes) provide a convenient way of identifying real atmospheric sensitivities. However,

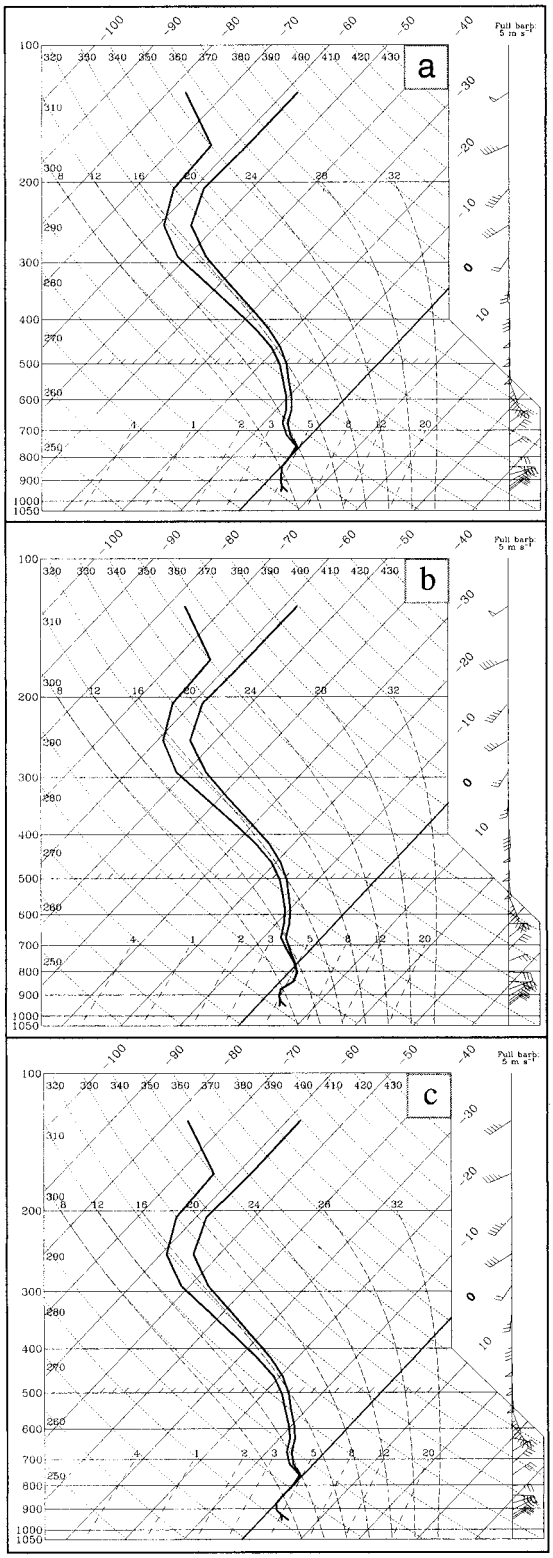

FIG. 12. Model-simulated soundings from CSV at the 8-h time, valid 2000 UTC 3 Feb 1998 for simulations with (a) the normal value for L_f, (b) L_f = O, and (c) double the normal value for L_f.

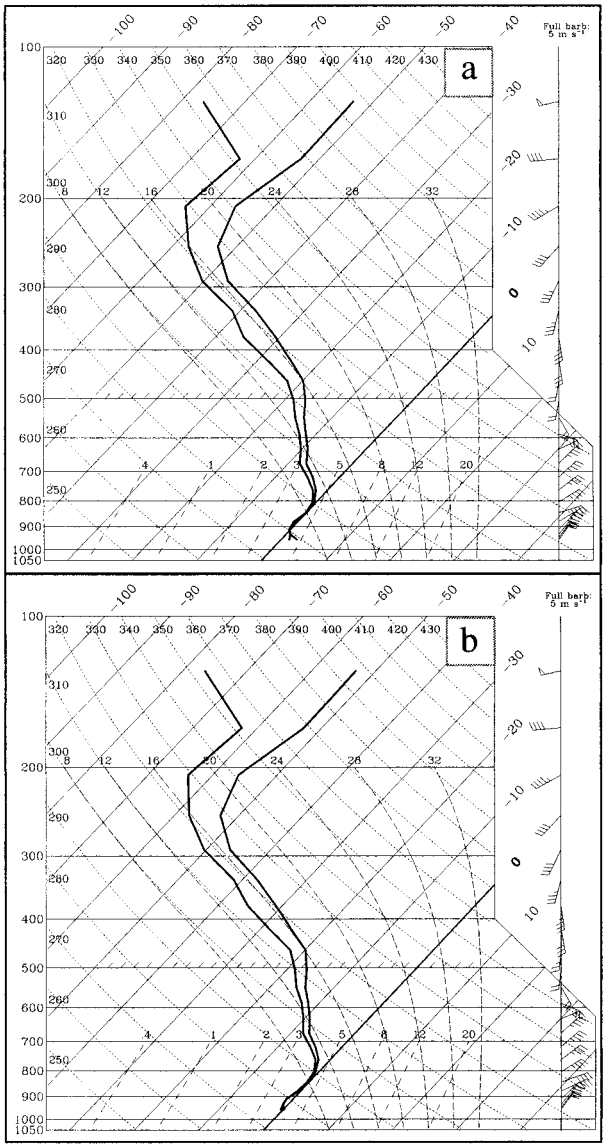

FIG. 13. Model-simulated sounding from CSV at the 12-h time, valid 0000 UTC 4 Feb 1998 for simulations with (a) the normal value for L_f, and (b) double the normal value for L_f.

because of nonlinear interactions in a numerical model, artificial adjustments to parameters controlling a single process tend to provide an ambiguous assessment of the true impact of that process or parameter (Stein and Alpert 1993). A diagnostic evaluation of predicted fields from a simulation with unmodified physics can provide a more clearly defined measure of the impact of a particular process. In this section we follow this more rigorous approach by extracting the temperature tendency associated with each physical process over CSV in order to assess the relative significance of the melting effect.

The temperature tendency at each grid point in MM5 is computed as the sum of seven separate physical processes: Horizontal (hadv) and vertical (vadv) advections, along with physical parameterizations for bulk latent heating (lath), vertical mixing/surface fluxes (vpbl), deep moist convection (conv), atmospheric radiation (arad), and horizontal mixing (hmix). This can be written schematically as

$$\left.\frac{\partial T}{\partial t}\right|_{\text{total}} = \left.\frac{\partial T}{\partial t}\right|_{\text{hadv}} + \left.\frac{\partial T}{\partial t}\right|_{\text{vadv}} + \left.\frac{\partial T}{\partial t}\right|_{\text{lath}} + \left.\frac{\partial T}{\partial t}\right|_{\text{vpbl}} + \left.\frac{\partial T}{\partial t}\right|_{\text{conv}} + \left.\frac{\partial T}{\partial t}\right|_{\text{arad}} + \left.\frac{\partial T}{\partial t}\right|_{\text{hmix}}. \quad (1)$$

Over CSV, parameterized deep convection was not activated during the simulation and temperature tendencies due to atmospheric radiation and horizontal mixing were negligible. Thus, we focus on the first four terms on the right-hand side of (1). Further, we isolate the melting effect from the total latent heating term. Time–height cross sections are plotted for the grid point nearest to CSV for these five dominant components, along with the total temperature tendency, in Fig. 14.

Appreciable warm (horizontal) advection is evident above about 600 mb for much of the 12-h period (Fig. 14a). This tendency is consistent with the 500-mb pattern shown in Fig. 2b and the airflow through the negatively tilted trough. In the lower troposphere, horizontal advective tendencies are negative, and larger in magnitude than one might have anticipated after an examination of the 1200 UTC 850-mb chart. One possible explanation for the large values is that horizontally differential latent cooling (i.e., evaporation and melting) created lower-tropospheric temperature gradients along the northeasterly inflow to eastern and middle Tennessee after 1200 UTC. This explanation is substantiated by the simulated temperature patterns at 850 mb valid 12 h later (Fig. 9b). The temperature gradient would have strengthened during the first few hours primarily owing to differential evaporation, but later in the period differential melting could have been important since precipitation amounts were greater in the model at points upstream (northeast) of CSV (Fig. 8a).

The strongest temperature tendencies associated with *vertical* motions are also concentrated above 600 mb. In particular, large negative values for the vertical advection term reflect strong upward motion in the conveyor-belt airstream above 600 mb. This ascent is accompanied by strong condensation/deposition (positive latent heat release in Fig. 14c). Below about 600 mb, however, subsidence prevails (indicated by *positive* values for the vertical advection term), and each pulse of subsidence is accompanied by a maximum in evaporative/sublimative cooling (cf. Figs. 14b and 14c). This direct correspondence suggests that evaporation/sublimation of precipitation falling from aloft effectively nudges the environment back toward saturation whenever subsidence produces a drying tendency over CSV. This pattern of subsidence warming/latent cooling is interrupted by a brief period of relatively weak upward

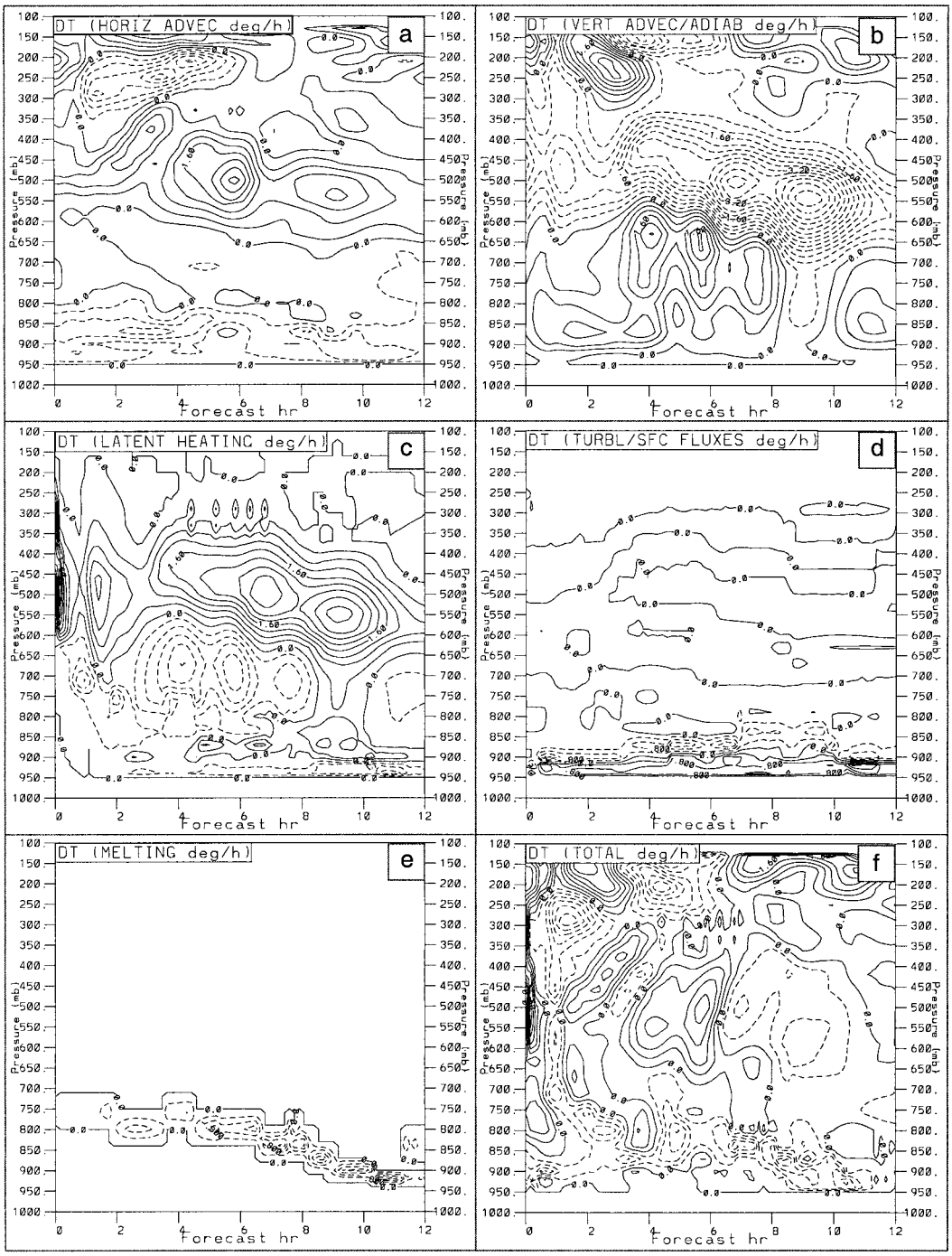

FIG. 14. Time–height cross sections of MM5-simulated temperature tendencies (contour interval = 0.4°C h^{-1}) over CSV from 1200 UTC 3 Feb 1998 to 0000 UTC 4 Feb 1998 due to (a) horizontal advection, (b) vertical advection/adiabatic effects, (c) latent heating (not including melting), (d) turbulent mixing/surface fluxes, (e) melting, and (f) all terms. Positive values are contoured with solid lines; negative values with dashed lines.

motion and condensation/deposition in the lower troposphere between the 8- and 10-h times.

The turbulent mixing/surface flux term produces a nearly continuous warming of the surface layer, a reflection of heat fluxes from the relatively warm ground (Fig. 14d). The parameterization responsible for this term also mixes strongly near the top of the planetary boundary layer over CSV, introducing a significant cooling tendency at times. Comparison of Figs. 14c and 14d between the 4- and 7-h times (1600–1900 UTC) sug-

gests that cooling associated with the turbulent mixing process may be supersaturating a layer between 900 and 850 mb (note the positive latent heating tendencies corresponding to the negative turbulent mixing/surface flux tendencies).

Finally, the melting term provides compelling evidence of the role played by melting in eroding the layer of above-freezing air and bringing snow levels down toward the surface over CSV (Fig. 14e). Specifically, melting is concentrated between 700 and 750 mb during the first 6 h (1200–1800 UTC) of the simulation, then steadily descends between 6 and 12 h (1800–0000 UTC), a period during which continuous moderate rainfall accumulated in the model. The magnitude of the melting term is sufficiently large that it typically dominates over other terms in the layer where it is active. The total temperature tendency term is clearly impacted strongly by the melting effect (cf. Figs. 14e and 14f).

This analysis could be done somewhat more rigorously by utilizing a Lagrangian perspective, wherein temperature tendencies for individual air parcels arriving at CSV at a specified time could be tracked backward in time. Indeed, it does appear that significant cooling occurred at upstream locations, as suggested above. That consideration notwithstanding, our diagnostic analysis leaves little doubt that neglect of the cooling effect of melting precipitation in a situation like this could easily cause a forecaster to dismiss the possibility of a significant snowfall.

It is worth noting that melting effects are included in operational numerical models. In fact, the authors were alerted to the potential emergence of an appreciable melting effect in this case by 0°C isothermal structures that appeared in routine Eta Model (Black 1994) forecasts. However, as with MM5, the isothermal layer in the Eta Model did not penetrate to the surface, probably because precipitation totals were significantly underpredicted by this model as well. In the next section, we deduce a set of important guidelines that can be used by forecasters to anticipate those situations in which the melting effect may become important.

4. Operational anticipation of significant melting effects

The potential impact of the melting effect in the type of environment examined here can be whittled down to a relatively simple ''rule of thumb.'' We begin in a manner similar to Wexler et al. (1954), with an expression of the first law of thermodynamics:

$$C_p\delta T + L_v\delta q_v - L_f\delta q_i = 0, \tag{2}$$

where C_p is the heat capacity of air at constant pressure (J kg^{-1}K^{-1}), δT is the change in air temperature (K), δq_v is the change in water vapor specific humidity (kg kg^{-1}), and δq_i is the change in ice mixing ratio, that is, the quantity of ice that melts (kg kg^{-1}). (As in our gridpoint analysis above, we consider latent heating/cooling effects as if they occur within a single column of the atmosphere, so that these effects may be considered to affect the local temperature field in a cumulative sense. In a stricter interpretation, the accumulation of latent heating effects would only be valid if we calculated these effects along a parcel path. However, for our purposes, this Eulerian framework should prove to be adequate.)

Since the melting effect becomes most prominent after evaporation rates become very small and the temperature approaches the wet-bulb temperature, we consider the impact of melting in an atmospheric column that is saturated with precipitation falling through from above. In this situation, the cooling associated with melting tends to produce a supersaturated environment and an adjustment back to saturation involves condensational warming, which partially offsets the melting effect. The amount of condensation that occurs, δq_v, depends on the rate of change of saturation specific humidity, q_s, as a function of temperature, so that (1) can be rewritten as

$$C_p\delta T + L_v\frac{\partial q_s}{\partial T}\delta T - L_f\delta q_i = 0 \tag{3}$$

and rearranging gives

$$\delta T = \frac{L_f\delta q_i}{C_p + L\upsilon\dfrac{\partial q_s}{\partial T}}. \tag{4}$$

This equation can be simplified considerably without much loss in precision. Consider the numerator on the right-hand side. If we assume that all of the precipitation melting in a column reaches the surface as precipitation, then δq_i can be expressed in terms of accumulated (liquid equivalent) precipitation. Specifically,

$$\delta q_i \approx \frac{-D}{\delta P}, \tag{5}$$

where D is the depth of the accumulated precipitation (cm) and δP is the pressure depth of the layer of the atmosphere that is affected (mb). The last term in the denominator on the right-hand side can be approximated as well. Noting that $\partial q_s/\partial T \approx (\varepsilon/P)(\partial e_s/\partial T)$, where $\varepsilon = 0.622$ and P is the ambient pressure in the same units as e_s, we can assume an ambient pressure of 950 mb and compute $\partial e_s/\partial T$ using the Clausius–Clapeyron equation (or a suitable empirical approximation) to arrive at $\partial q_s/\partial T \approx 2.91 \times 10^{-4}$ kg kg^{-1} K^{-1}. Finally, using standard values for L_f, L_v, and C_p, we can write

$$\delta T \approx -193\frac{D}{\delta P}, \tag{6}$$

which can then be rearranged to give

$$D \quad \text{(cm)} \approx \frac{-\delta T\times\delta P}{193}. \tag{7}$$

This expression gives the rainfall amount that would eliminate a melting layer with ''positive area'' on a thermodynamic diagram given by $\delta T \times \delta P$, where δP is the pressure depth of the above-freezing layer (mb) and δT is the mean temperature difference between the freezing point and the wet-bulb temperature of the environment (i.e., the negative of the mean wet-bulb temperature in °C) in the layer. Alternatively, we could express D in units of inches, rounding off to give this simple expression:

$$D \quad \text{(in.)} \approx \frac{-\delta T \times \delta P}{500}. \tag{8}$$

This indicates, for example, that a melting layer with a depth of 100 mb and a mean wet-bulb temperature of 1°C could be eliminated with approximately 0.2 in. of rain. If we apply (7) to the 1200 UTC sounding from BNA, using a mean wet-bulb temperature of 2.5°C over the lowest 200 mb, it suggests that the melting layer could be eliminated by 2.6 cm of precipitation. This is slightly more than the amount observed at BNA (Fig. 8), but the surface temperature never reached the freezing point and our model diagnostics indicated that there was also weak cold advection in the lower troposphere that would have augmented the melting effect, so the rule of thumb is consistent with observations in this case.

As emphasized in the introduction, the melting effect, although significant in an absolute sense, typically has a relatively small impact on the net temperature tendency over a deep layer. In particular, it usually has a much smaller effect on temperature changes than tendencies due to advective processes (i.e., both horizontal and vertical advections). Consequently, strong consideration of the melting effect as a potentially significant player in determining precipitation type should be reserved for those situations in which lower-tropospheric temperature advections are weak. In general, this is most likely to be the case in the northwest quadrant of a surface cyclone, particularly a mature system in which system-relative easterly flow aloft can result in a significant influx of moisture and generation of snow at midlevels.

5. Summary and conclusions

Melting snowflakes extract heat from the atmosphere, typically over a layer several hundred meters deep. As a result, the melting effect can lower the level to which subsequent flakes can penetrate. In some cases, the intensity of this process can have a significant impact in determining where snow reaches the ground and where it does not. Although melting effects can have important dynamical consequences as well, in this study we have focused on the problem of quantifying the potential magnitude of the melting effect and providing guidelines for anticipating those situations when it makes the difference between rain and snow at the surface.

A ''surprise'' snow event from February 1998 was used to demonstrate a situation in which the melting effect can be the key ingredient in causing a changeover from rain to snow. During the afternoon and evening of 3 February 1998, forecasters at both the SPC and local National Weather Service offices in Tennessee did not anticipate the rapid cooling of the lower troposphere and heavy snowfall that followed several hours of moderately heavy rainfall over east-central Tennessee and surrounding regions. In hindsight, numerous indicators pointed to atmospheric cooling caused by melting snow as a potentially important factor in the lowering of snow levels and the eventual changeover from rain to snow at the surface.

A mesoscale model (MM5) was used to simulate this event and confirm, through diagnostic analysis of model output, that the melting effect extracted enough heat from the lower troposphere to completely eliminate the melting layer and allow snow to reach the surface. The configuration of MM5 used for this study was rather modestly sophisticated, by today's standards. This configuration was intentionally chosen because of its accessibility. In particular, this version of MM5 is run daily, in a semioperational forecast mode, at the NSSL and is readily available and relatively simple to utilize in an operational environment. It proved to be more than adequate for this study.

In addition to diagnosing the significance of the melting effect for this particular meteorological event, we have provided guidelines to assist forecasters in identifying when it may become a significant factor in other events. Situations where the following three criteria are met may warrant a consideration of the melting effect in the forecast process.

1) *Low-level temperature advection is weak.* Given that the melting effect is usually a second-order contributor to the atmospheric temperature tendency compared to other adiabatic and diabatic processes, forecasters should focus their attention on areas where these other processes are minimized in the lower troposphere. An example would include the northwest quadrant of a mature extratropical cyclone, where both temperature advections and vertical motions are often relatively weak in low levels.
2) *Steady rainfall of at least moderate intensity is expected for several hours.* To a first approximation, the cumulative effect of melting is directly proportional to the accumulated rainfall. Cooling due to melting will be strongest where precipitation rates are the highest.
3) *Surface temperatures are generally within several degrees of freezing at the onset of the event.* If precipitation rates are expected to be light, the melting effect is not likely to play an important role unless temperatures are not far from the freezing level. Warmer temperatures will require higher precipitation rates.

When these three conditions are anticipated in an area, forecasters should consider the potential impact of melting precipitation on local temperature profiles. If, in addition, anticipated precipitation totals come close to or exceed the approximate threshold value given by (7) or (8), forecasters should strongly consider the possibility that snow levels will reach the surface.

Finally, we wish to emphasize that this study was greatly facilitated by the collocation of the SPC and NSSL facilities. The first two authors were both present at the SPC winter weather forecast desk as the surprise snowstorm blossomed around 0000 UTC 4 February 1998. Their keen interest in this event was fueled by the excitement that it generated, the forecasting challenge that it presented, and the obvious need to understand it better. In their effort to explain the unfolding evolution of events, they both committed to an exchange of time, resources, and data that would have been much less likely to come together if not for the collocated facilities. Thus we present this study as an example of how collaboration between operational forecasters and research scientists can be promoted and facilitated by the collocation of operational and research facilities.

Acknowledgments. The authors wish to thank John Cortinas (CIMMS/NSSL), Chuck Doswell (NOAA/NSSL), Bob Johns (NOAA/SPC), David Schultz (CIMMS/NSSL), and two anonymous reviewers for their thoughtful reviews of this manuscript.

REFERENCES

Atlas, D., R. Tatehira, R. C. Srivastava, W. Marker, and R. E. Carbone, 1969: Precipitation-induced mesoscale wind perturbations in the melting layer. *Quart. J. Roy. Meteor. Soc.,* **95,** 544–560.

Black, T. L., 1994: The new NMC mesoscale Eta Model: Description and forecast examples. *Wea. Forecasting,* **9,** 265–278.

Braun, S. A., and R. A. Houze, 1995: Melting and freezing in a mesoscale convective system. *Quart. J. Roy. Meteor. Soc.,* **121,** 55–77.

Carbone, R. E., 1982: A severe frontal rainband. Part I: Stormwide hydrodynamic structure. *J. Atmos. Sci.,* **39,** 258–279.

Carlson, T. N., 1991: *Mid-Latitude Weather Systems.* HarperCollins Academic, 507 pp.

Dudhia, J., 1989: Numerical study of convection observed during the winter monsoon experiment using a mesoscale two-dimensional model. *J. Atmos. Sci.,* **46,** 3077–3107.

——, 1993: A nonhydrostatic version of the Penn State/NCAR mesoscale model: Validation tests and simulation of an Atlantic cyclone and cold front. *Mon. Wea. Rev.,* **121,** 1493–1513.

Ferber, G. K., C. F. Mass, G. M. Lackmann, and M. W. Patnoe, 1993: Snowstorms over the Puget Sound lowlands. *Wea. Forecasting,* **8,** 481–504.

Findeisen, W., 1940: The formation of the 0°C-isothermal layer and fractocumulus under nimbostratus. *Meteor. Z.,* **6,** 882–888.

Gedzelman, S., and E. Lewis, 1990: Warm snowstorms: A forecaster's dilemma. *Weatherwise,* **43,** 265–270.

Grell, G. A., J. Dudhia, and D. R. Stauffer, 1994: A description of the fifth generation Penn State/NCAR mesoscale model (MM5). NCAR Tech Note NCAR/TN-398+STR, 138 pp.

Kain, J. S., and J. M. Fritsch, 1993: Convective parameterization for mesoscale models: The Kain-Fritsch scheme. *The Representation of Cumulus Convection in Numerical Models, Meteor. Monogr.,* No. 46, Amer. Meteor. Soc., 165–170.

Lumb, F. E., 1961: The problem of forecasting the downward penetration of snow. *Meteor. Mag.,* **90,** 310–319.

Marwitz, J., 1983: The kinematics of orographic airflow during Sierra storms. *J. Atmos. Sci.,* **40,** 1218–1227.

——, and J. Toth, 1993: The Front Range blizzard of 1990. Part I: Synoptic and mesoscale structure. *Mon. Wea. Rev.,* **121,** 402–415.

Steenburgh, W. J., C. F. Mass, and S. A. Ferguson, 1997: The influence of terrain-induced circulations on wintertime temperature and snow level in the Washington Cascades. *Wea. Forecasting,* **12,** 275–285.

Stein, U., and P. Alpert, 1993: Factor separation in numerical simulations. *J. Atmos. Sci.,* **50,** 2107–2115.

Stewart, R. E., 1984: Deep 0°C isothermal layers within precipitation bands over southern Ontario. *J. Geophys. Res.,* **89,** 2567–2572.

——, 1992: Precipitation types in the transition region of winter storms. *Bull. Amer. Meteor. Soc.,* **73,** 48–51.

Szeto, K. K., and R. E. Stewart, 1997: Effects of melting on frontogenesis. *J. Atmos. Sci.,* **54,** 689–702.

Wexler, R., R. Reed, and J. Honig, 1954: Atmospheric cooling by melting snow. *Bull. Amer. Meteor. Soc.,* **35,** 48–51.

Zhang, D.-L., and R. A. Anthes, 1982: A high resolution model of the planetary boundary layer—Sensitivity tests and comparisons with SESAME-79 data. *J. Appl. Meteor.,* **21,** 1594–1609.